Extended data figures

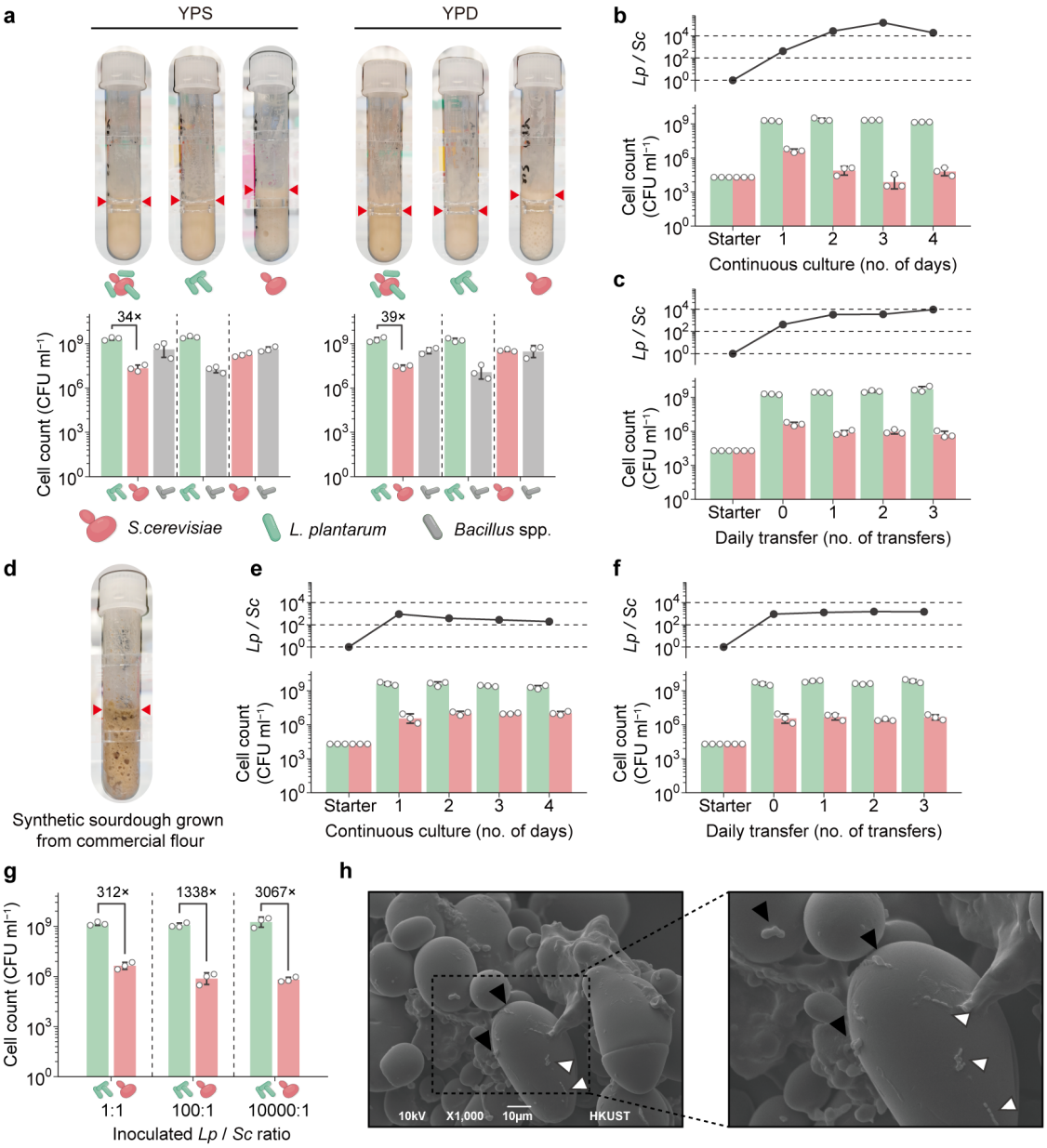

Extended Data Fig. 1: Inoculation conditions to determine the texture and composition of synthetic starter.

(**a**) Cell counts and images of synthetic starter grown from YPD and YPS (mean ± sd, n = 3 starters). The red triangular arrows indicate the fermentation height of the synthetic starter. Grey bars indicate uninoculated *Bacillus* spp. in the starter, likely originating from the gluten product. (**b** and **c**) Cell counts and ratio of *L. plantarum* NC8 to *S. cerevisiae* (*Lp* / *Sc*) over days of continuous culture (**b**) and daily transfer (**c**) (cell count represented by mean ± sd, ratio represented by mean value, n = 3 starters). (**d**) Image of synthetic sourdough starter grown from commercial flour. (**e** and **f**) Cell counts and *Lp* / *Sc* ratio over days of continuous culture (**e**) and daily transfer (**f**) with commercial flour (cell counts represented by mean ± sd, ratio represented by mean value, n = 3 starters). (**g**) Cell counts of the synthetic starter grown

from different inoculation ratios (cell counts represented by mean ± sd, n = 3 starters). (**h**) Representative SEM imaging of the synthetic starter. Black arrow: *S. cerevisiae* cells; white arrow: *L. plantarum*.

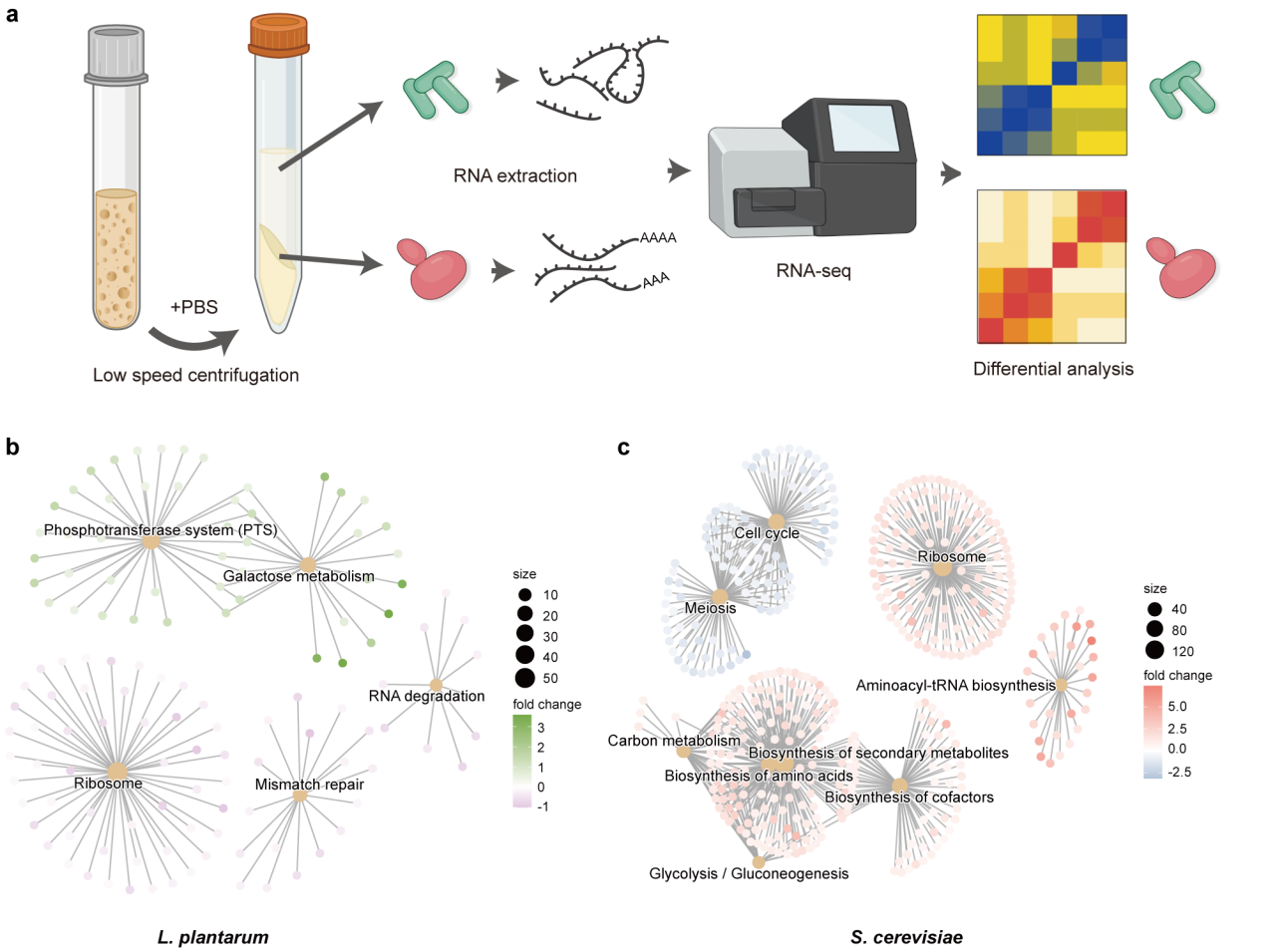

Extended Data Fig. 2: Transcriptomic analysis to reveal molecular interactions between *L. plantarum* and *S. cerevisiae* in synthetic starter.

(**a**) Schematic of transcriptomic analysis workflow. (**b** and **c**) Gene set enrichment assay of RNA-seq results for *L. plantarum* (**b**) and *S. cerevisiae* (**c**) under co-culture conditions compared with mono-culture conditions.

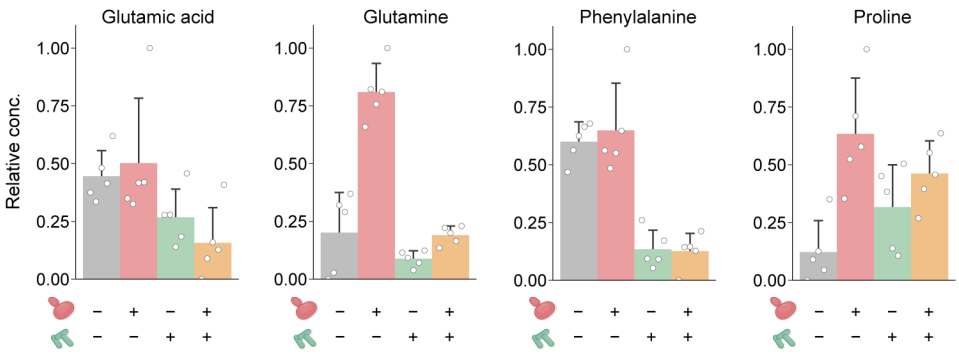

Extended Data Fig. 3: Metabolomic analysis of synthetic sourdough starter.
Analysis of the relative concentration of glutamic acid, glutamine, phenylalanine and proline in synthetic starter from blank medium, *L. plantarum* mono-culture, *S. cerevisiae* mono-culture, and co-culture (mean ± sd, n = 5 starters).

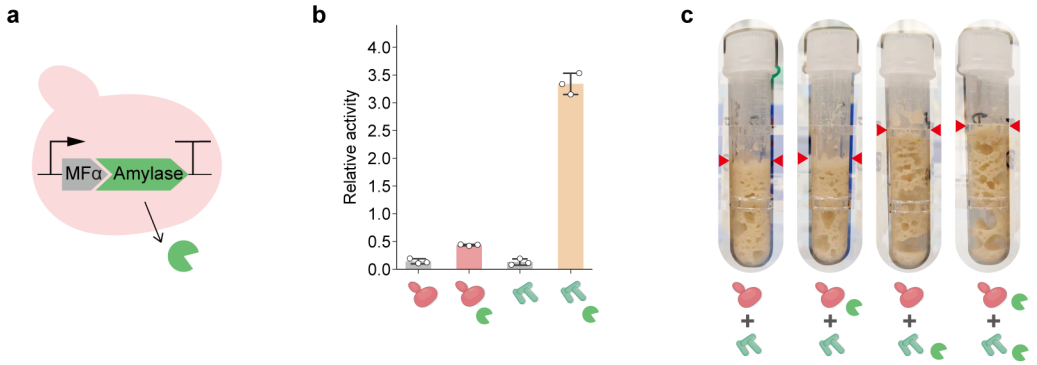

Extended Data Fig. 4: Characterizing amylase-secreting *S. cerevisiae*.
(**a**) Schematic of the engineered amylase-secreting *S. cerevisiae* strain. (**b**) Characterization of amylase-secreting capacity of the *S. cerevisiae* strain and comparison with *S. cerevisiae* wild-type strain, *L. plantarum* wild-type, and the ylF201 amylase-secreting *L. plantarum* strains (mean ± sd, n = 3 independent cultures). (**c**) Representative images from the combinatorial co-culturing of *L. plantarum* and *S. cerevisiae* wild-type or amylase-secreting strain.

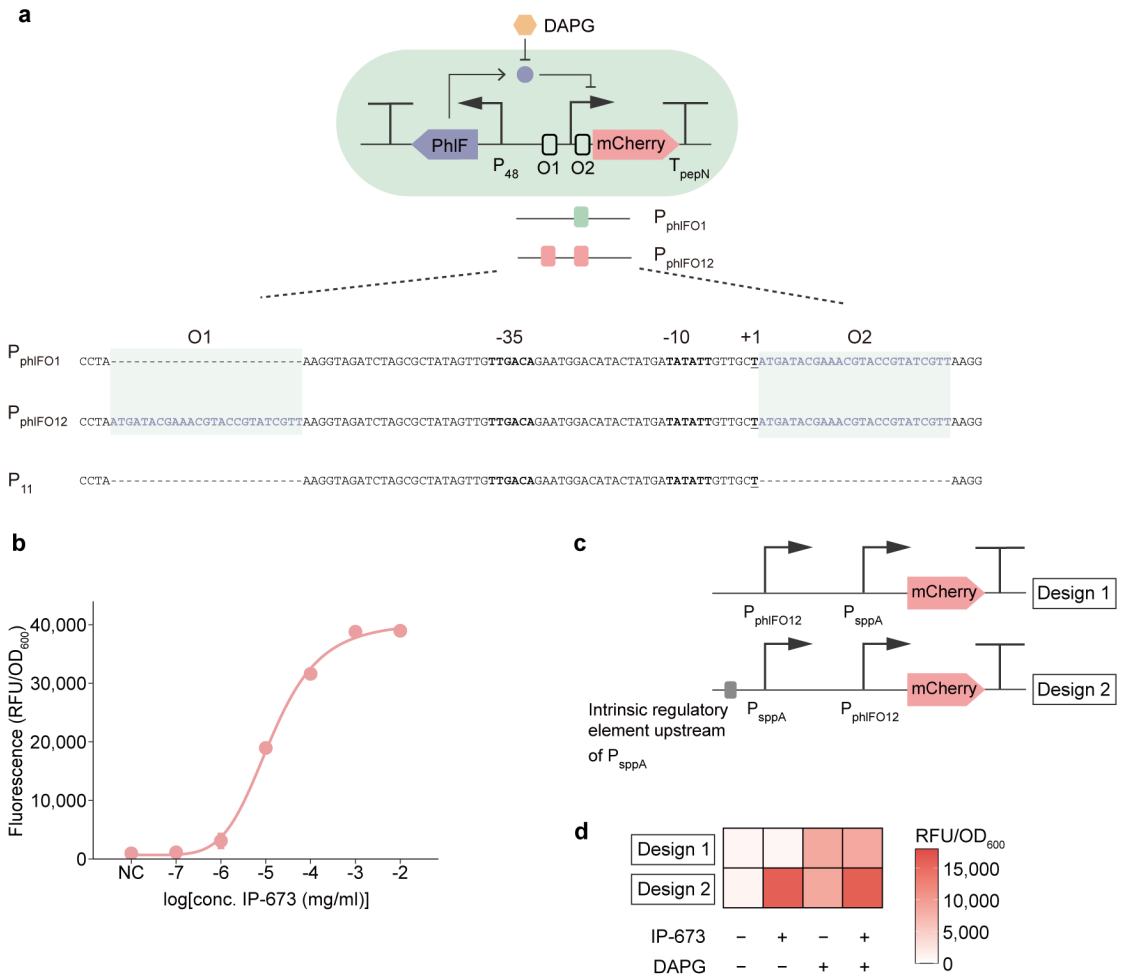

Extended Data Fig. 5: Design and characterization of DAPG/IP-673 OR-gate in *L. plantarum*.

(**a**) Design of PhlF-binding promoters. PhlF operator sites were inserted in various regions (O1 or O2) of the P_{11} promoter. (**b**) Dose-response properties of IP-673 peptide-inducible system in *L. plantarum* (mean ± sd, n = 3 independent cultures). (**c**) Design of DAPG/IP-673 OR-gate *L. plantarum* strains. (**d**) Characterization of the OR-gate in MRS broth with fluorescence output (mean, n = 3 independent cultures).

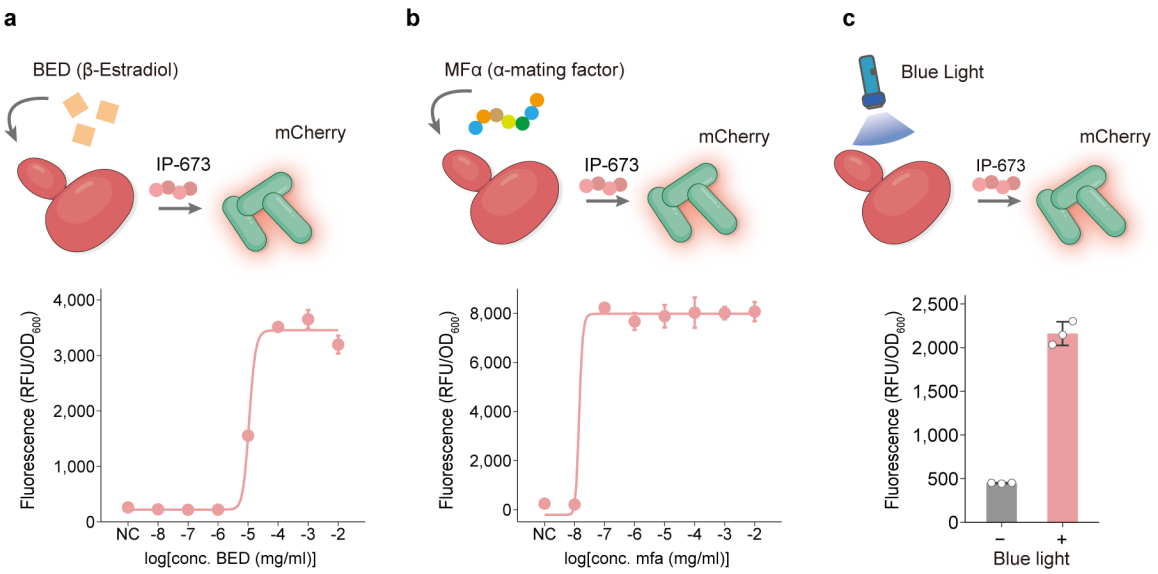

Extended Data Fig. 6: Characterization of the communication system with mCherry fluorescence as reporter.

(**a**-**c**) The responses of engineered consortia to various signals – (**a**) BED, (**b**) MFα (**c**) Blue light (mean ± sd, n = 3 independent cultures). NC, negative control.

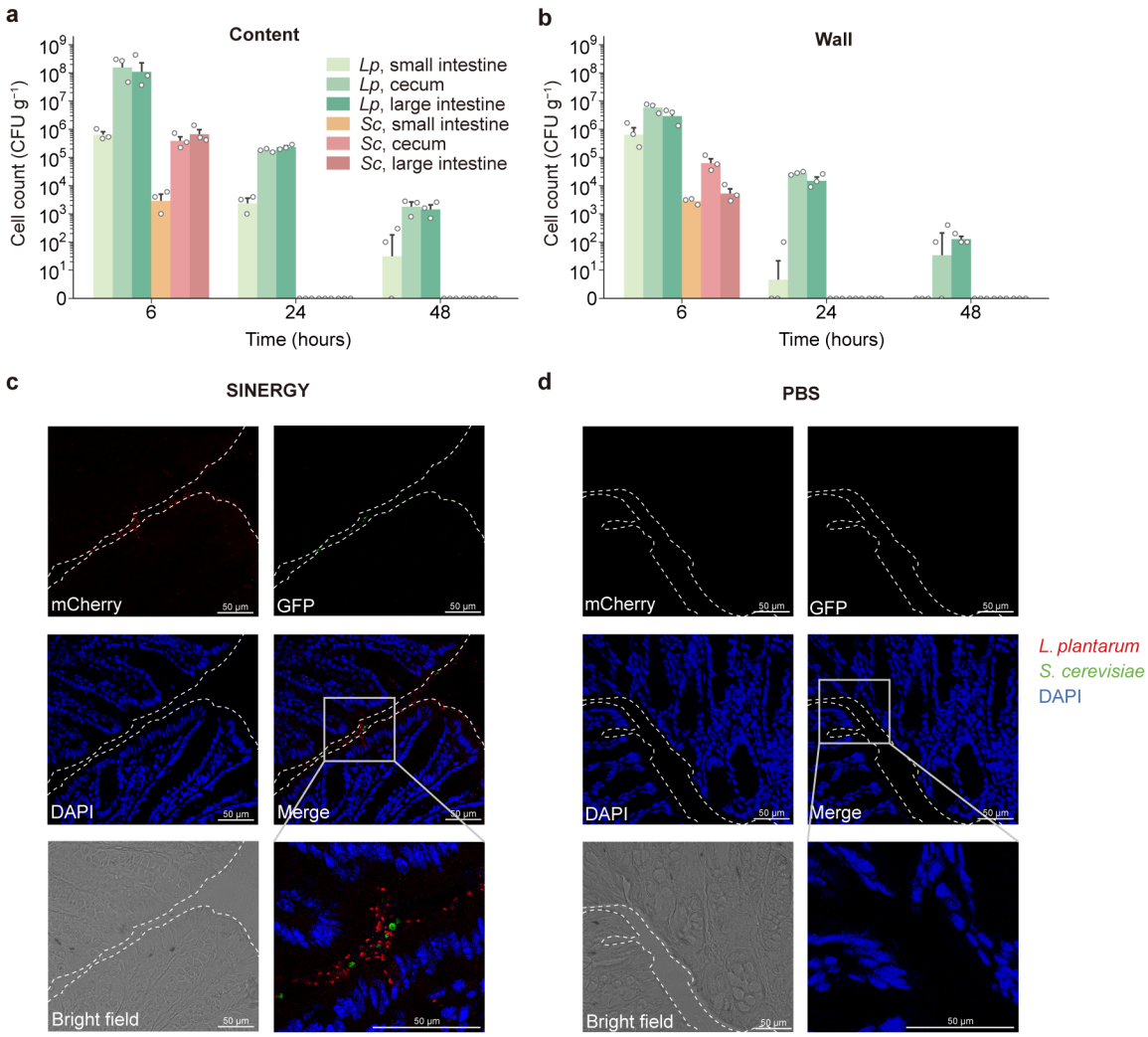

Extended Data Fig. 7: Viability of *L. plantarum* and *S. cerevisiae* delivered by SINERGY in the murine gut.

(**a** and **b**) Microbial cell counts in gut contents (**a**) and on walls (**b**) (mean ± SEM, n = 3 mice). (**c** and **d**) Additional confocal visualization of fluorescent microorganisms in the colon of mice administered with SINERGY (**c**) compared with PBS (**d**).

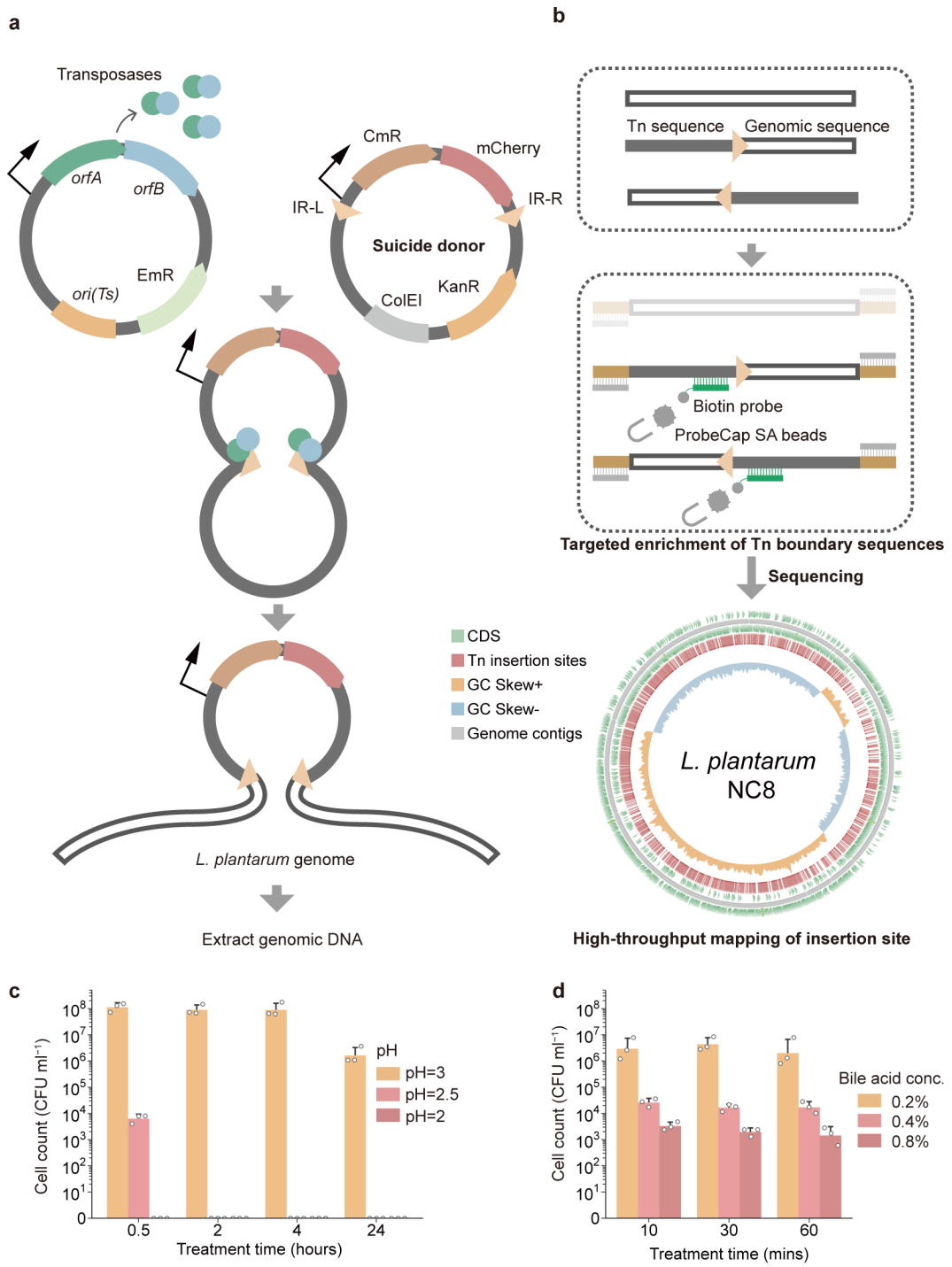

Extended Data Fig. 8: Construction of *L. plantarum* Tn-mutagenesis system.
(**a**) Schematic of the Tn-mutagenesis system in *L. plantarum*. A thermo-sensitive plasmid for constitutively expressing transposases is first introduced into *L. plantarum*, followed by electroporation of a suicide transposon donor that cannot replicate in *L. plantarum* (**Methods**). The integrated colonies that maintain CmR (chloramphenicol resistance) are selected. (**b**) Targeted enrichment sequencing for identifying the Tn-inserted genomic features. (**c** and **d**) Preliminary exploration of screening conditions for low pH treatment (**c**) and bile acid concentration (**d**) (mean ± sd, n = 3 independent experiments).

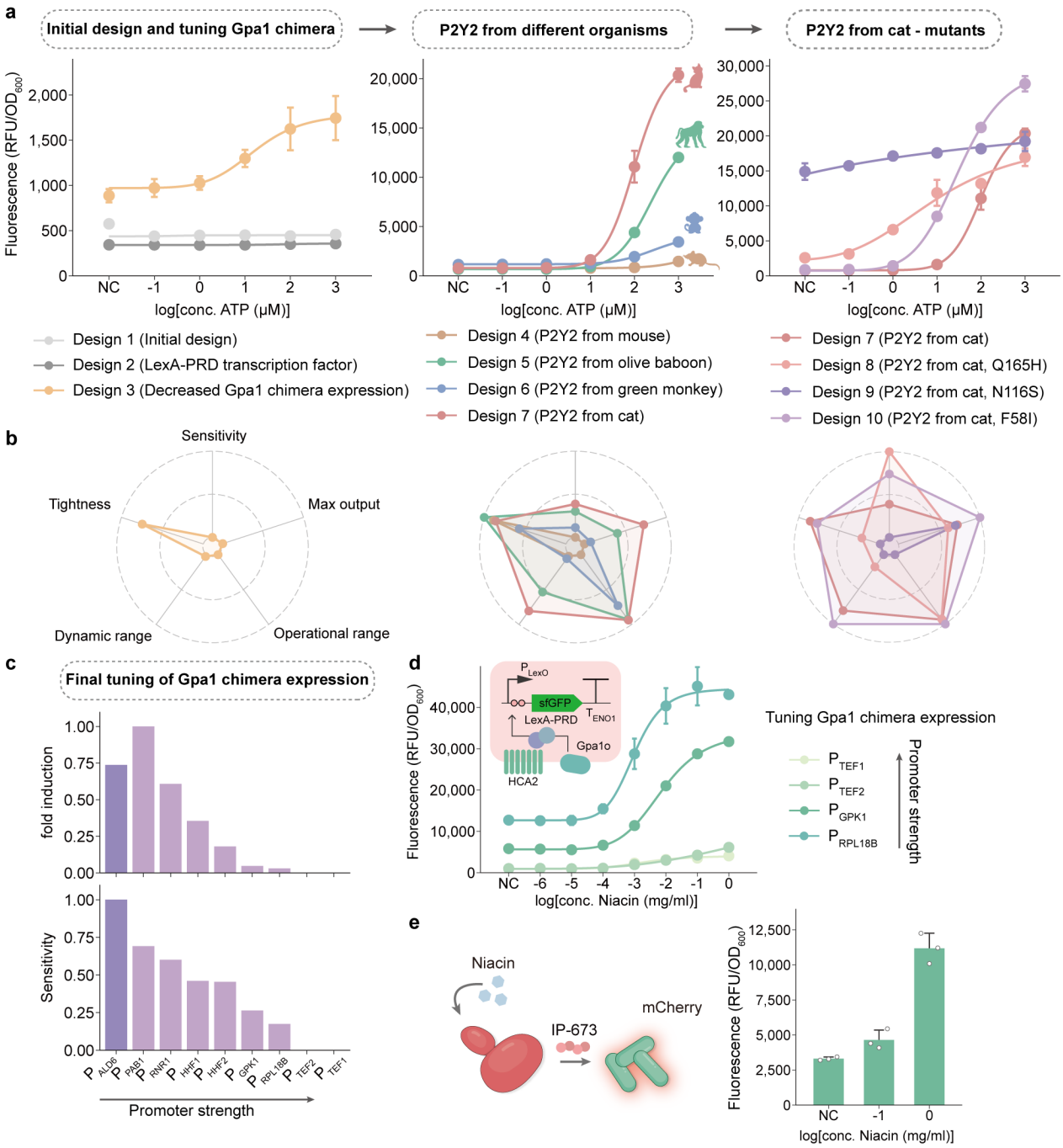

Extended Data Fig. 9: Construction and optimization of yeast GPCR-based sensor. (**a** and **b**) Dose-response curve (**a**) and radar chart (**b**) of the yeast eATP sensor constructs (mean ± sd, n = 2 or 3 independent cultures). (**c**) Characterization of eATP sensor fold induction and sensitivity with various promoters for Gα chimera expression (mean). (**d**) Dose-response curve of yeast GPCR-based niacin sensor designs (mean ± sd, n = 3 independent cultures). (**e**) Characterization of niacin sensing consortia with *L. plantarum* expressing mCherry as output (mean ± sd, n = 3 independent cultures). NC, negative control.

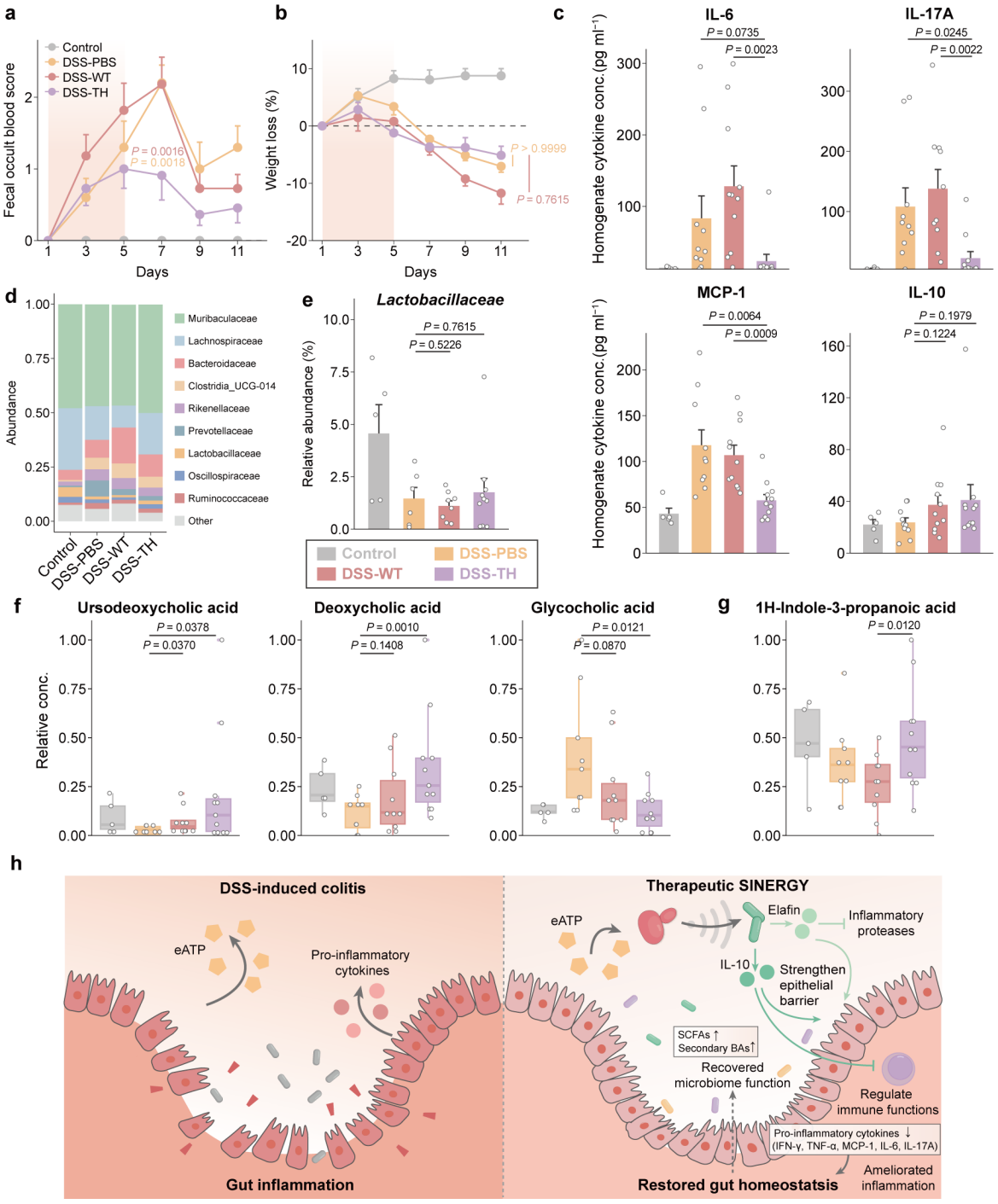

Extended Data Fig. 10: Response of DSS-induced colitis to therapeutic SINERGY, consisting of engineered consortia, as revealed by restored microbiota and metabolite levels.

(**a** and **b**) Fecal occult blood score (**a**) and body weight loss (**b**) of each group of mice (mean ± SEM, statistical significance was determined by two-way ANOVA, P value representing comparison of DSS-TH group versus DSS-PBS or DSS-WT group, n = 5 mice for Control group, n = 10 for DSS-PBS group, n = 11 for DSS-WT and DSS-TH group). (**c**) Additional cytokine levels of colon homogenate (mean ± SEM, statistical significance was determined by unpaired two-sided t-test, n = 5 samples for Control group, n = 10 for DSS-PBS group, n

= 11 for DSS-WT and DSS-TH group). (**d**) Relative abundance of bacteria classified at a family-level taxonomy. (**e**) Relative abundance of the *Lactobacillaceae* family (mean ± SEM, statistical significance was determined by unpaired two-sided t-test, n = 5 samples for Control group, n = 7 for DSS-PBS group, n = 8 for DSS-WT and n = 10 DSS-TH group). (**f** and **g**) Additional bile acid metabolites (**f**) and indole-3-propanoic acid (**g**) of colon content (statistical significance was determined by unpaired two-sided t-test, n = 5 samples for Control group, n = 9 for DSS-PBS group, n = 10 for DSS-WT and n = 11 DSS-TH group). (**h**) Schematic of the multiple functions of therapeutic SINERGY in DSS-induced colitis.